Supplementary Information (SI) for Inorganic Chemistry Frontiers.

Tm^{3+}-Mediated Energy Bridge in Lead-Free Double Perovskites: Suppressing Multiphonon Relaxation for Multifunctional Photonic Applications

Jiaqi Zhao[a], Zheng Fu[a], Kejie Li[a], Mengmeng Dai[a], Zhiying Wang[b, *],Guiying Liang[c], Yanling Wei[c, *]and Zuoling Fu[a,*]

[a.] *Key Laboratory of Physics and Technology for Advanced Batteries, College of Physics, Jilin University, Changchun 130012, China. E-mail：zlfu@jlu.edu.cn*

[b.] *Ministry of Education Key Laboratory for Cross-Scale Micro and Nano Manufacturing, Nanophotonics and Biophotonics Key Laboratory of Jilin Province, School of Physics, Changchun University of Science and Technology, Changchun, 130022, China. E-mail: zhiyingw@cust.edu.cn*

[c.] *School of Data Science and Artificial Intelligence, Jilin Engineering Normal University, Changchun 130052, China. E-mail: weiyanling@jlenu.edu.cn*

To explicitly define the luminescence *LIR* models, we have completed the detailed descriptions of the transitions and equations below:

(i) LIR_1: Defined as the intensity ratio of the emission from Er^{3+}: $^2H_{11}/_2 \rightarrow {}^4I_{15}/_2$ (530 nm) to Tm^{3+}: $^1G_4 \rightarrow {}^3H_6$ (475 nm), i.e.,

$LIR_1 = \frac{I_{530\ nm}}{I_{475\ nm}}$. This non-thermally coupled level (non-TCL) model follows the empirical fitting equation:

$$LIR_1 = A_1 + B_1 \cdot exp\left(\frac{C_1}{T}\right)$$

Where A_1, B_1 and C_1 are represented as constants, respectively, and T is the absolute temperature (Figs. 11a and 12a).

(ii) LIR_2: Defined as the ratio of Er^{3+}:$^2H_{11}/_2 \rightarrow {}^4I_{15}/_2$ (530 nm) to Er^{3+}:$^4S_3/_2 \rightarrow {}^4I_{15}/_2$ (550 nm), i.e., $LIR_2 = \frac{I_{530\ nm}}{I_{550\ nm}}$. This thermally coupled level (TCL) model adheres to the Boltzmann distribution:

$$LIR_2 = A_2 \cdot exp\left(-\frac{\Delta E}{K_B T}\right)$$

Where A_2 is represented as a constant, ΔE = 0.0984 eV (derived from the energy gap between $^2H_{11}/_2$ and $^4S_3/_2$), K_B is the Boltzmann constant, and the fitting yields $R^2 > 0.99$ (Figs. 11b and 12b).

(iii) LIR_3: Defined as the ratio of Er^{3+}:$^2H_{11}/_2 \rightarrow {}^4I_{15}/_2$ (530 nm) to Er^{3+}:$^4F_9/_2 \rightarrow {}^4I_{15}/_2$ (660 nm), i.e., $LIR_3 = \frac{I_{530\ nm}}{I_{660\ nm}}$. The empirical equation is used in this mixed-mode model:

$$LIR_3 = A_3 + B_3 \cdot exp\left(\frac{C_3}{T}\right)$$

Where A_3, B_3 and C_2 are represented as constants, respectively, with $R^2 > 0.99$ (Figs. 11c and 12c).

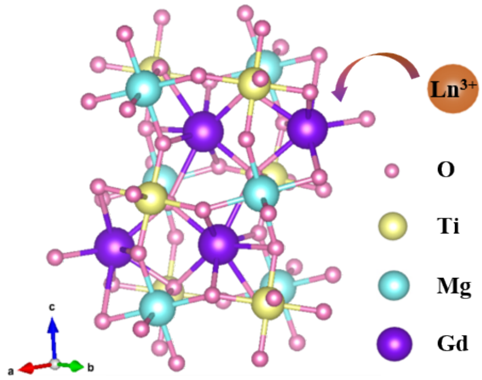

Fig. S1 Crystal structure of Ln^{3+}-doped GMTO double perovskite.

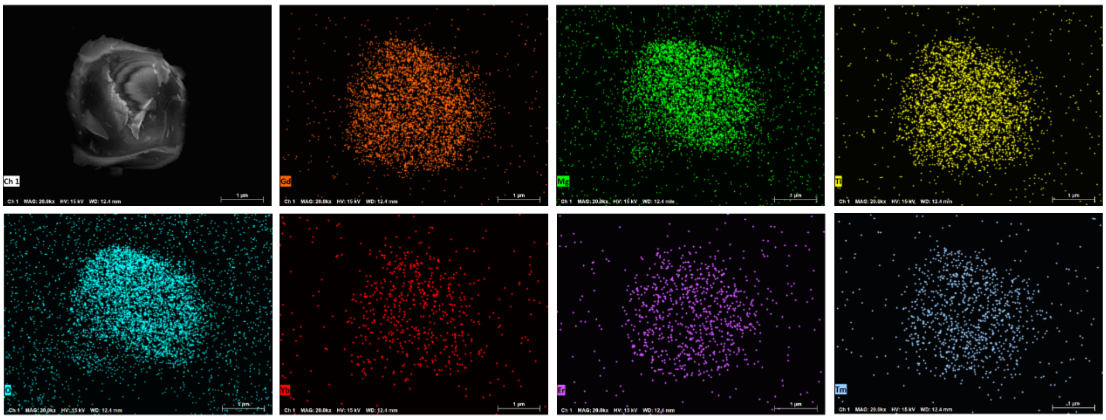

Fig. S2 FE-SEM image and elemental mapping images of the GMTO: 7% Yb^{3+}, 2% Er^{3+}, 3%Tm^{3+} sample.

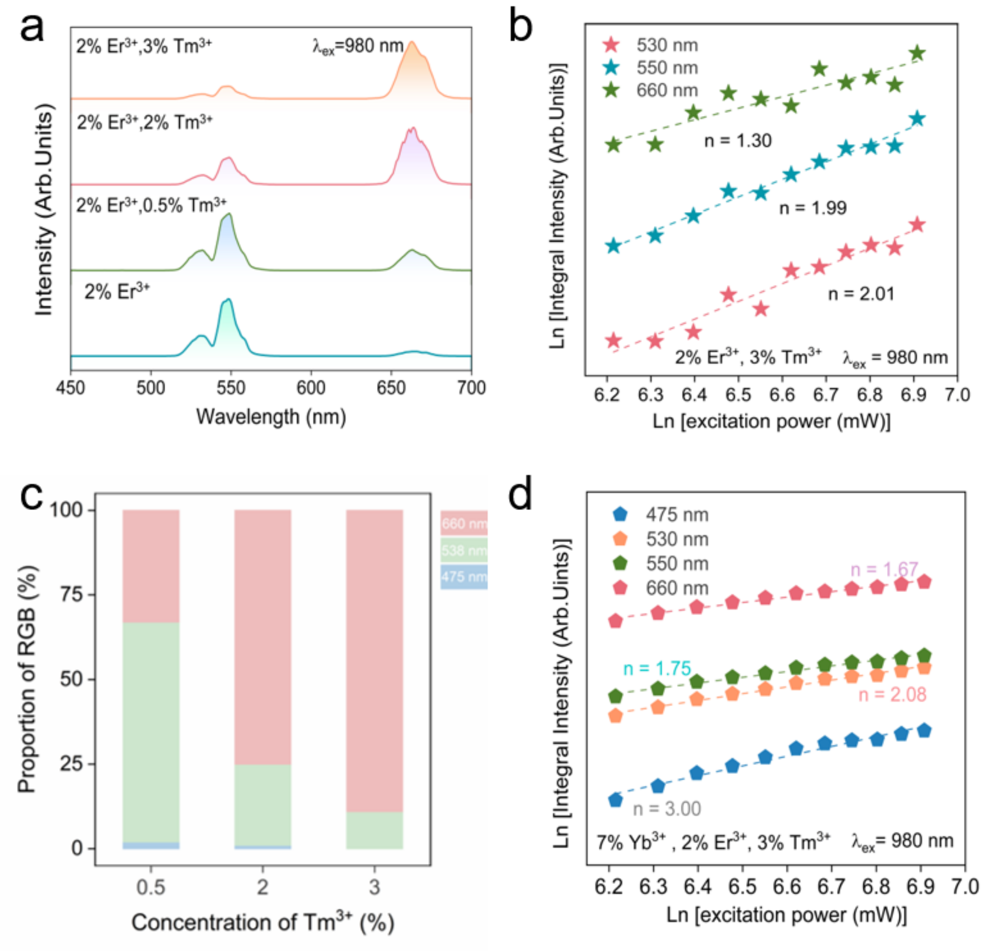

Fig. S3 (a) UC emission spectra of GMTO: 2% Er^{3+}, xTm^{3+}(x = 0-3%) under 980 nm excitation. (b) Calculated power dependence of the UC luminescence and linear fittings about GMTO: 2%Er^{3+}, 3%Tm^{3+}. (c) Proportion of GMTO: Yb^{3+}, Er^{3+}, Tm^{3+} integral intensity with different concentrations of Tm^{3+}. (d) Calculated power dependence of the UC luminescence and linear fittings about GMTO: 7%Yb^{3+}, 2%Er^{3+}, 3%Tm^{3+}.

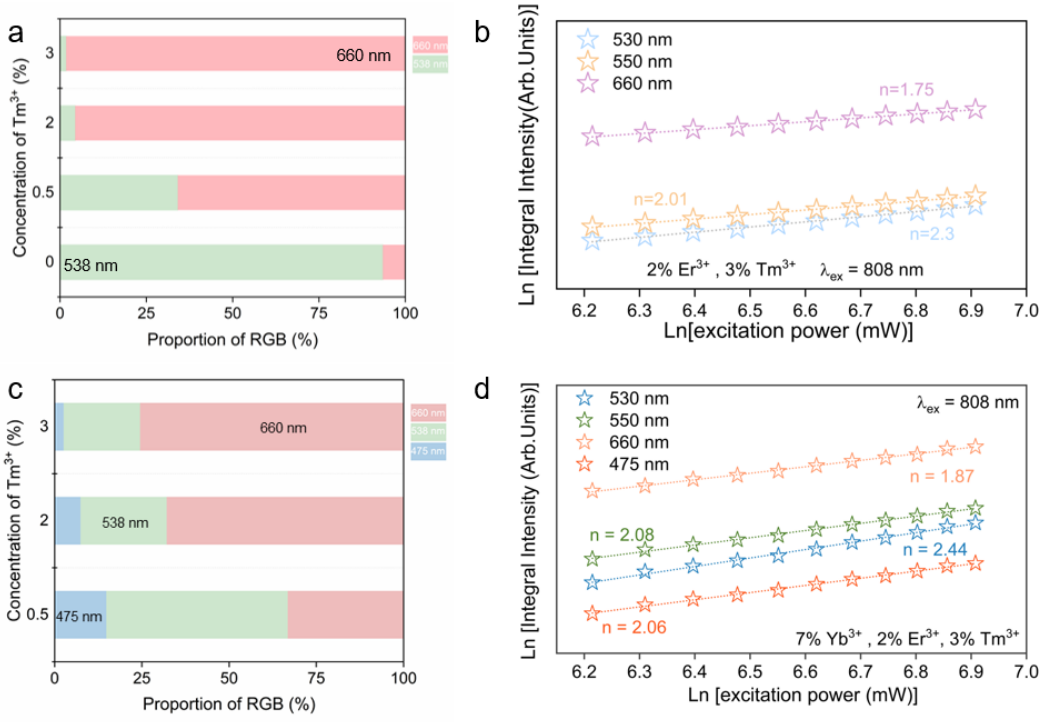

Fig.S4 (a) Proportion of GMTO: 2%Er^{3+}, Tm^{3+} integral intensity with different concentrations of Tm^{3+}. (b) Calculated power dependence of the UC luminescence and linear fittings of GMTO: 2%Er^{3+}, 3%Tm^{3+}. (c) Proportion of GMTO: 7Yb^{3+}, 2%Er^{3+}, $y$$Tm^{3+}$($x$ = 0.5-3%) integral intensity. (d) Calculated power dependence of the UC luminescence and linear fittings of GMTO: 7%Yb^{3+}, 2%Er^{3+}, 3%Tm^{3+}.

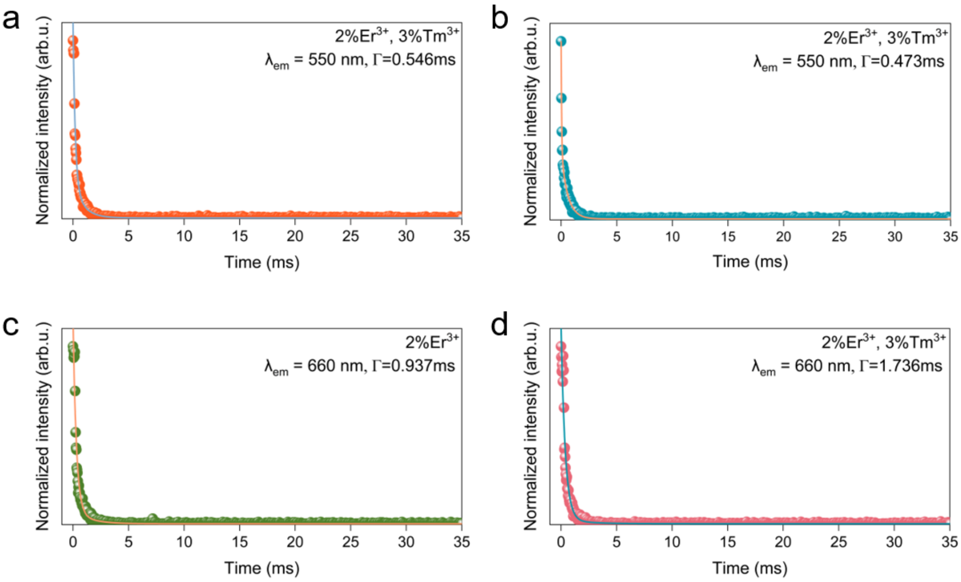

Fig.S5 (a and b) UC decay lifetimes of green emission at 550 nm of Er^{3+} in the GMTO: 2%Er^{3+} and GMTO: 2%Er^{3+}, 3%Tm^{3+} under 808 nm excitation, respectively. (c and d) UC decay lifetimes of red emission at 660 nm of Er^{3+} in the GMTO: 2%Er^{3+} and GMTO: 2%Er^{3+}, 3%Tm^{3+} under 808 nm excitation, respectively

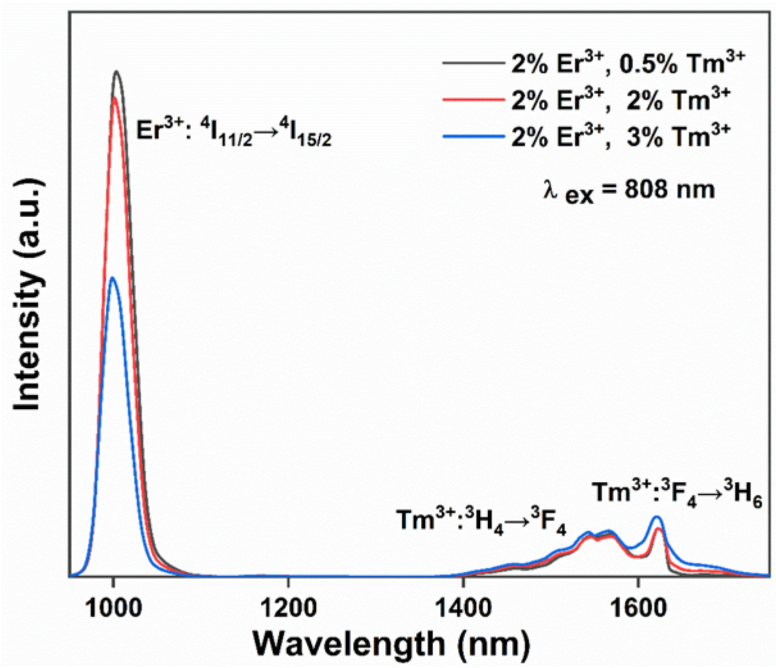

Fig. S6 NIR emission spectra of Er^{3+}, xTm^{3+}(x = 0-3%) co-doped system upon 808 nm excitation.

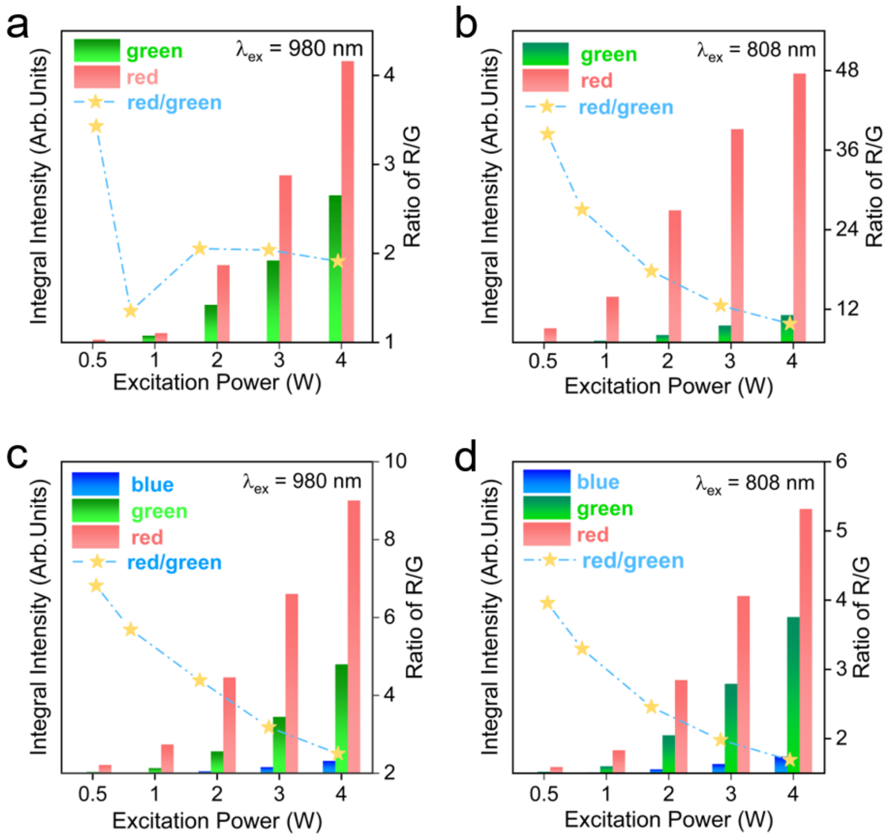

Fig. S7 UC emission integrated intensity and red-to-green ratio of the corresponding samples as a function of laser power.

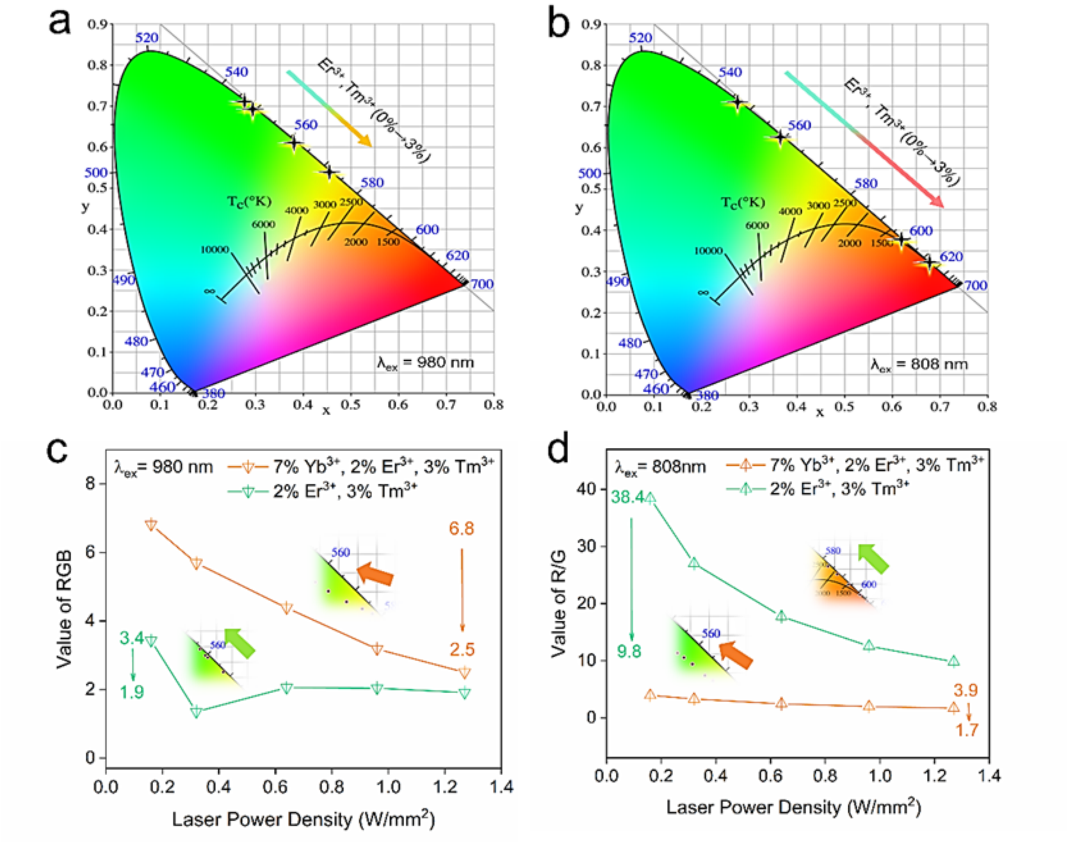

Fig. S8 (a, b) CIE chromatic coordinates of the UC emission in the GMTO: 2% Er^{3+}, 0.5%Tm^{3+} phosphor by varying concentration of Tm^{3+} under 980/808 nm excitation. (c, d) R/G emission ratio of GMTO: Er^{3+}, xTm^{3+}(x = 0-3%) and GMTO: Yb^{3+}, Er^{3+}, xTm^{3+}(x = 0.5-3%) with the variation of laser power density.

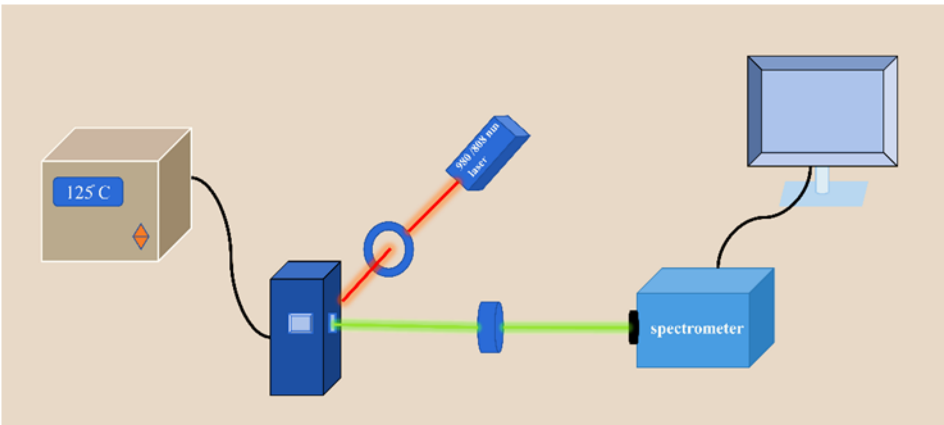

Fig. S9 Schematic diagram of the experimental equipment for temperature sensing measurements.

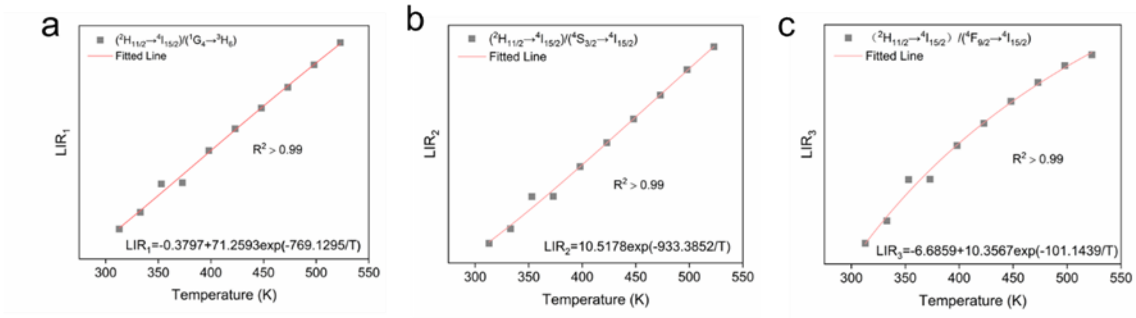

Fig. S10 (a-c) Temperature-dependent *LIR* values of GMTO:7%Yb^{3+}, 2%Er^{3+}, 0.5%Tm^{3+} upon 980 nm excitation.

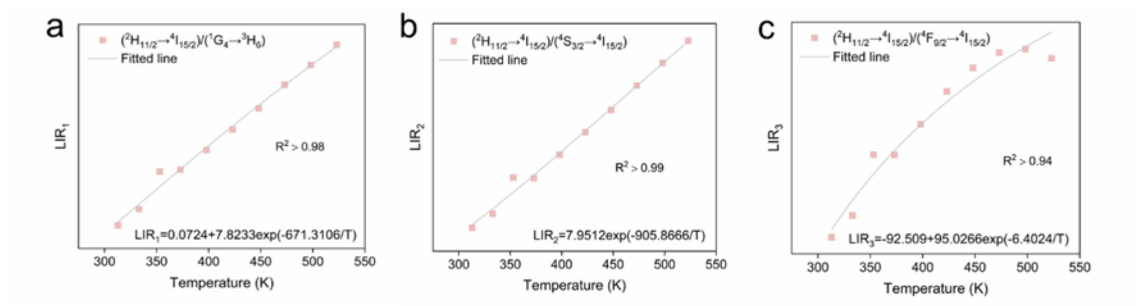

Fig. S11 (a-c) Temperature-dependent *LIR* values of GMTO:7%Yb^{3+}, 2%Er^{3+}, 0.5%Tm^{3+} upon 808 nm excitation.

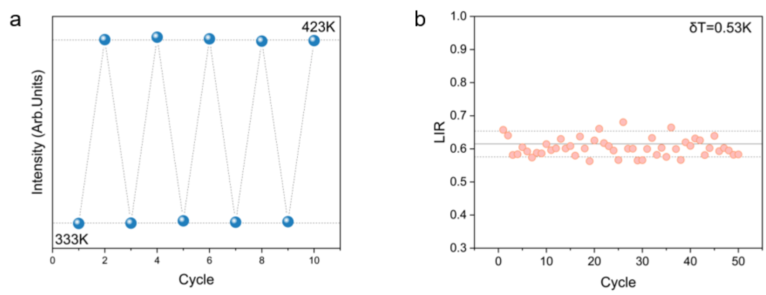

Fig. S12 (a) Thermal cycling stability (10 cycles between 333 and 423 K) of the GMTO:7%Yb^{3+}, 2%Er^{3+}, 0.5%Tm^{3+} under 980 nm excitation. (a) Repeatability tests (25 cycles at 333 K) of the LIR_2 signals under 980 nm excitation.

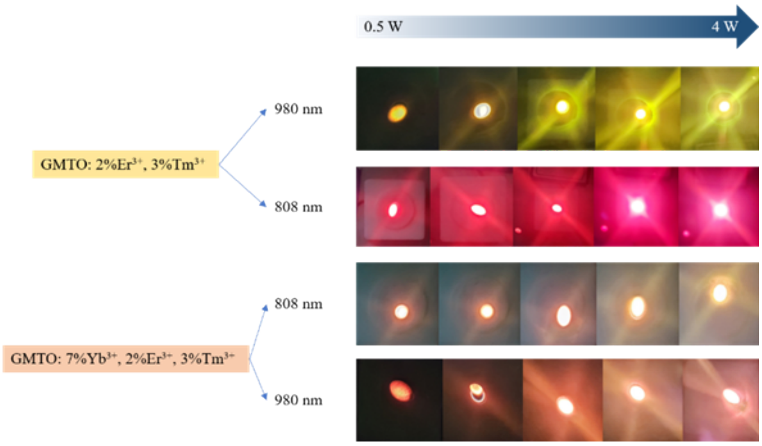

Fig. S13 Images of GMTO: 2%Er^{3+}, 3%Tm^{3+} and GMTO: 7%Yb^{3+}, 2%Er^{3+}, 3%Tm^{3+} under different excitation wavelengths and powers.

Table S1. Refinement Results of Gd_2MgTiO_6: 7% Yb^{3+}, 2% Er^{3+}, 3% Tm^{3+}.

Refinement Results of GMTO					
Space Group P 21/n	Symmetry Monoclinic	a=5.36428 Å b=5.60566 Å c=7.68344 Å	V=231.043 Å^3	α=90 β=89.87543 γ=90	R_{wp}=2.44% R_p=1.95% Chi^2=1.70%

Table S2. Summary of the S_r value corresponding to the Ln^{3+}-doped *LIR* thermometers.

Phosphors	λ_{ex}(nm)	Transitions	Temperature(K)	S_r(%K^{-1})	Refs
$Na_3Gd(VO_4)_2$: Yb^{3+}/Er^{3+}	980	$^2H_{11/2}$,$^4S_{3/2}\rightarrow{}^4I_{15/2}$	291-578	0.83	[32]
TeO_2-ZnO-BaO: Yb^{3+}/Ho^{3+}	980	$^5F_5/^5F_4$,$^5S_2\rightarrow{}^5I_8$	303-503	0.41	[42]
$NaLuF_4$: Ho^{3+}/Yb^{3+}	980	$^5F_1$,$^5G_6/^5F_{2,3}$,$^3K_8\rightarrow{}^5I_8$	390-780	0.83	[43]
YOF: Tm^{3+}/Yb^{3+}	980	$^3H_4\rightarrow{}^3H_6$	190-300	0.12	[33]
Ca_2MgWO_6: Er^{3+}/Yb^{3+}	980	$^2H_{11/2}/^4F_{9/2}\rightarrow{}^4I_{15/2}$ $^2H_{11/2}/^4S_{3/2}\rightarrow{}^4I_{15/2}$	303-573	0.47 0.92	[44]
$Ba_5Gd_8Zn_4O_{12}$: Yb^{3+}/Tm^{3+}	980	$^1G_{4(1,2)}\rightarrow{}^3H_6$	300-510	0.56	[34]
Gd_2MgTiO_6: $Yb^{3+}/Er^{3+}/Tm^{3+}$	980	LIR_1 LIR_2 LIR_3	313-523	0.84 0.95 0.95	This work
	808	LIR_1 LIR_2 LIR_3	313-523	0.64 0.92 1.03	This work